UNIVERSAL PLL STRATEGY FOR SENSORLESS SPEED AND POSITION ESTIMATION OF PMSM

Georges El-Murr, Damian Giaouris, and J.W. Finch

***Abstract*—the implementation of the Phase Locked Loop (PLL) structured observer in high frequency signal injection schemes requires tuning of the PI controller to lock on the rotor position. The PI controller is tuned depending on the Signal to Noise Ratio (SNR) which is related to the amount of saliency/anisotropy presented in the machine, the amplitude and phase of the incoming modulated carrier signal. Thus, in case any of the mentioned factors changes then the PI has to be retuned again, otherwise it will loose track. In this paper a new PLL structure is suggested to avoid any disturbance that affects the demodulation and detection process. The new PLL scheme is totally independent of any machine parameters except the saliency/anisotropy, which is essential to obtain the rotor speed and position information.**

***Index Terms*— High-frequency signal injection, Phase-Locked Loop, Sensorless control, Surface-Mounted Permanent Magnet Synchronous Motor**

I. INTRODUCTION

THE main objective of *sensorless control* is to achieve the same control performance as *vector control* without using speed or position sensor [1]. Such a sensor can be the most expensive and fragile component in the whole electric drive. Sensorless techniques Fig.1 are divided into two classes, those using the fundamental properties or model of the machine [2-5] and those exploiting subsidiary features often called anisotropies based model [6-9].

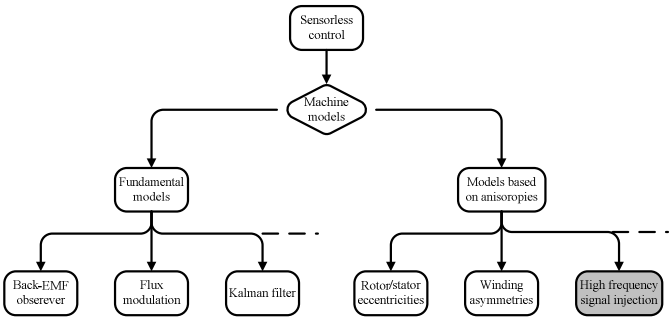

Fig.1: Categories of sensorless control techniques

Manuscript received, 2008. G. El-Murr, D. Giaouris and J.W. Finch are with the Electrical Drives Group, School of Electrical, Electronic & Computer Engineering, Newcastle University, NE1 7RU, UK.

S*ensorless control* of a PMSM has become more and more acceptable in industrial applications due to the large amount of research effort that has been spent in developing reliable, low-cost PMSM drives. The simplest fundamental model methods are based on rotor flux position estimation, by integrating the back-EMF [10]. Such an approach is very simple but fails at low and zero speed. In general, low speed operation is critical for such fundamental based methods, since the estimated rotor flux can be very sensitive to stator resistance variations, and measurement noises. In addition, sensorless schemes that are based on the application of sophisticated identification procedures (such as flux observers, Kalman filter [1-3] etc.) allow, with some limitations very low speed operation, but can be too complex and expensive to be used in practical systems. Other estimation techniques can be based on stator phase voltage third harmonics or spatial phenomena inherent within the machine, such as slot harmonics, rotor/stator eccentricities, and winding asymmetries. However all these approaches can fail at zero speed for lack of useful information.

Signal injection schemes [11-15] can be more efficient, at low and zero speed, than any other sensorless estimation scheme. Such methods have the capability to provide accurate position and speed estimation without requiring information about the motor parameters. This is due to the presence of saliency/anisotropy in the machine. The saliency/anisotropy is the inductance difference between direct-inductance l_d and quadrature-inductance l_q and it is due to either the asymmetric structure of the machine or the flux induced magnetic saturation due to the fundamental excitation. The interaction between the injected high frequency signal and the spatial variations in the machine inductances produces an amplitude-modulated signal containing useful information attached to the carrier frequency. The demodulation and extraction of this information constitute the main interest of this paper, which is presented as follows:

In section II a theoretical background of the conventional modulation, heterodyning demodulation, and the PLL observers implemented in rotating and alternating signal injection schemes. Section III covers the proposed demodulation as well as the speed and position estimation method. Finally, results of the estimated and actual rotor speed and position are presented in section IV to validate the proposed method and compare it with the conventional schemes.

II. HIGH FREQUENCY SIGNAL INJECTION: MODULATION AND DEMODULATION

A. Rotating and Alternating Signal Modulation

In general high frequency signal injection methods, Fig. 2, consist of 3 main parts:

1. Signal injection or modulating signal
2. Demodulation process
3. Speed and position estimation

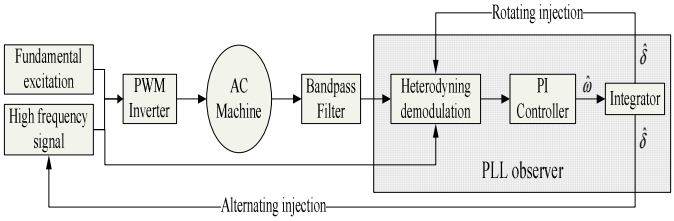

Fig.2: Block diagram of the high frequency signal injection schemes

There are 2 ways of injecting a high frequency signal into the PMSM to find the rotor speed and position. The injected signal can be a 3-phase balanced signal (rotating injection) [11, 13, 14] or a single phase injected signal in the estimated rotor position (alternating injection) [15-17] . The injected high-frequency (carrier frequency) components are considered to be sufficiently higher than the rotor speed and much lower than the inverter switching frequency. In most cases, the carrier frequency ω_c is chosen to be between (500 Hz - 2 kHz). However, the injected voltage amplitude is best made small to reduce the effect of the additional current on the control scheme.

The information related to the rotor speed and position is attached to the negative components (rotating injection) (1) or negative and positive components (alternating injection) (2) of the high frequency resultant signal:

$$i_c = i_{c\alpha} + j i_{c\beta} = -jA_c\left(L_{dq}e^{j(\omega_c)t} + l_{dq}e^{-j(\omega_c - 2\delta_r)}\right) \quad (1)$$

$$i_c = -j\frac{A_c}{2}\begin{pmatrix} L_{dq}e^{j\omega_c t+\hat{\delta}_r} - l_{dq}e^{j\omega_c t-\hat{\delta}_r+2\delta_r} \\ -L_{dq}e^{-j\omega_c t+\hat{\delta}_r} + l_{dq}e^{-j\omega_c t-\hat{\delta}_r+2\delta_r} \end{pmatrix} \quad (2)$$

where, $L_{dq} = l_d + l_q$, $l_{dq} = l_d - l_q$, and $A_c = \dfrac{V_c}{2(\omega_c - \omega_r)l_d l_q}$

Such information can be extracted using a bandpass filter centred at the carrier frequency with a bandwidth defined according to the rated speed of the machine. Usually, the bandpass filter is followed by a heterodyning demodulation method and a Phase Locked Loop (PLL) structure based speed and position observer that will be discussed in the next section.

B. Open Loop demodulation

The carrier frequency current signal presented in (1) consists of positive and negative sequence components. Only the negative sequence component has the information related the rotor position.

To separate the rotor speed information apart from the carrier frequency, the resultant high frequency current (1) is multiplied by another signal that rotates at an angular velocity equal to $\omega_c - 2\hat{\omega}_r$.

$$i_c^{\omega_c - 2\hat{\omega}_r} = -jA_c\left(L_{dq}e^{j(2\omega_c t - 2\hat{\delta}_r)} + l_{dq}e^{j(2\delta_r - 2\hat{\delta}_r)}\right) \quad (3)$$

The resultant signal represents the difference between estimated and actual rotor position (4) and can be extracted by using a low pass filter:

$$LPF\left(i_c^{\omega_c - 2\hat{\omega}_r}\right) = -jA_c\left(l_{dq}e^{j(2\delta_r - 2\hat{\delta}_r)}\right) \quad (4)$$

For a small speed or position difference between the actual and estimated position $sin\Delta\delta = \Delta\delta$, and the real part of (4) can be rewritten as:

$$\mathrm{Re}\left(LPF\left(i_c^{\omega_c - 2\hat{\omega}_r}\right)\right) = A_c l_{dq}\Delta\delta \quad (5)$$

where $\Delta\delta = \delta_r - \hat{\delta}_r$, is the error between the actual and estimated rotor position.

To minimise the error, an open loop PLL strategy Fig.3 (the output of the PLL is not fed-back to the input carrier signal) is applied and (5) can be used as a corrective error to lock on the rotor position

The Laplace transfer function *H(s)* of the open loop PLL based structure is:

$$\frac{\theta_o(s)}{\theta_i(s)} = H(s) = \frac{A_c l_{dq} F(s)}{1 + A_c l_{dq} F(s)} \quad (6)$$

where $\theta_i(s)$ is the phase of the input signal i_c, $\theta_o(s)$ is the phase of the oscillator, and *F(s)* represents the Laplace transfer function of the PI controller

$$F(s) = \frac{K_p s + K_i}{s} \quad (7)$$

Therefore the combination of (6) and (7) results in the basic loop equation:

$$H(s) = \frac{A_c l_{dq}\left(K_p s + K_i\right)}{s^2 + A_c l_{dq} K_p s + A_c l_{dq} K_i} \quad (8)$$

Because the highest power of *s* in the denominator function is 2, the loop is known as a "second order loop". Thus, the response of the system is characterised by the natural frequency ω_n, and the damping ratio ξ:

$$\omega_n = \sqrt{A_c l_{dq} K_i} \quad (9)$$

$$\zeta = \frac{1}{2}K_p\sqrt{\frac{A_c l_{dq}}{K_i}} \quad (10)$$

Assuming ω_n and ζ are set to achieve the appropriate response by tuning the proportional K_p and integrator K_i gains of the controller. The remaining factor is the current amplitude, which depends on the injected voltage, the carrier frequency and the amount of saliency/anisotropy in the machine. The injected voltage and frequency are usually chosen to increase the SNR and improve the dynamic of the PLL and are fixed. However, this choice is limited by the inverter power, switching frequency and the application speed range. In addition, the amount of saliency/anisotropy varies depending on the operating conditions of the machine. Therefore, it is required to determine the machine inductances l_{dq} in order to normalise the resultant modulated signal ic and avoid any parameter variation that may affects the estimation process

[18] . However, the PI gains can compensate to some extent the amplitude variation of the carrier current signal but this may affect the accuracy of the estimator (delayed position response, more ripples in the speed response).

As a result the application of the conventional open loop PLL scheme is still dependent on some machine parameters, and the observer estimated speed and position response can be deflected from the actual position at certain operating condition.

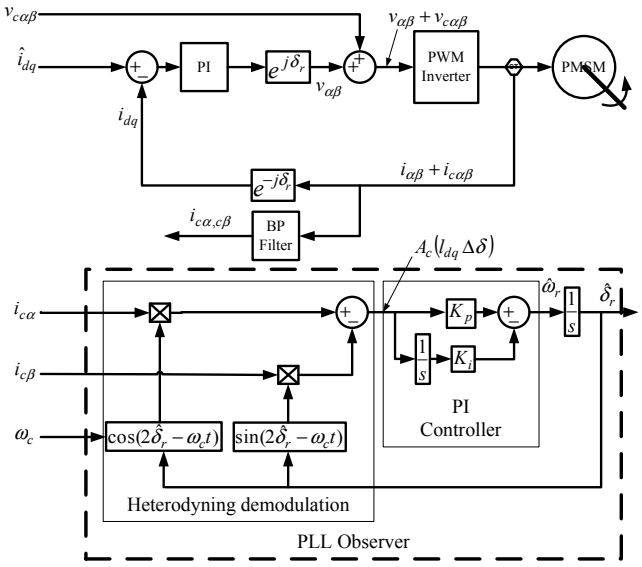

Fig.3: Open Loop PLL speed and position estimator structure

C. Closed Loop demodulation

The purpose of injecting a sine wave signal in the estimated reference frame is to generate a positive as well as negative current sequence components containing information about the rotor angular position (2). There are two possible way to inject the carrier voltage either in the d-axis or q-axis. Between the two injection algorithms, injecting the fluctuating high frequency voltage signal only in the d-axis is preferable with regard to torque ripple.

Using this type of injection, the demodulation algorithm requires the high frequency current (2) to be transferred to the estimated reference frame in negative direction at approximate carrier frequency:

$$i_c^{\omega_c t+\hat{\delta}} = i_c e^{-\left(j\omega_c t+\hat{\delta}\right)} \tag{11}$$

The transformed resultant current contains high frequency current which is rejected by a lowpass filter and the remaining of the signal is represented as follows:

$$LPF\left(i_c^{\omega_c t+\hat{\delta}}\right) = -j\frac{A_c}{2}\left(L_{dq} - l_{dq}\, e^{j(-2\hat{\delta}_r+2\delta_r)}\right) \tag{12}$$

For a small misalignment between the estimated and actual angle, the current response (12) containing the useful information can be simplified and rewritten as:

$$LPF\left(i_c^{\omega_c t+\hat{\delta}}\right) = -j\frac{A_c}{2}\left(L_{dq} - l_{dq}\,\Delta\delta\right) \tag{13}$$

Equation (13) represents the real part of the complex equation (12), which is proportional to the angle error $\Delta\delta$. This can be used to track the rotor position by a closed loop PLL strategy shown in Fig.4. However, this method is subjected to the same problem of parameter dependency as the open loop strategy discussed previously.

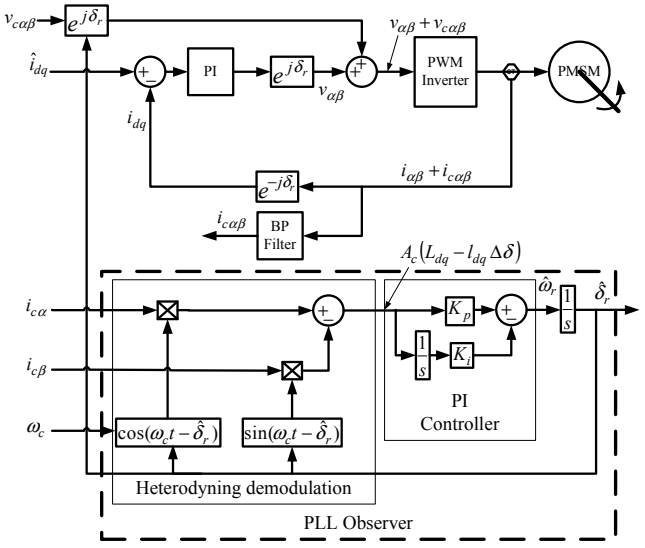

Fig.4: Closed Loop PLL speed and position estimator structure

III. PROPOSED SPEED AND POSITION OBSERVER

The saliency/anisotropy presented in the PMSM can help to make the machine itself act as a resolver. Thus, by injecting a rotating voltage signal into the PMSM machine a current signal, which is described by (1), has to be demodulated. The real and imaginary part of that signal are multiplied (14) and then by using a first order low pass filter the following can be obtained:

$$i_{c\alpha} \times i_{c\beta} = \begin{bmatrix} \left(K_1 \sin(\omega_c t) + K_2 \sin(\omega_c t - 2\omega_r t)\right)\times \\ \left(-K_1 \cos(\omega_c t) - K_2 \cos(\omega_c t - 2\omega_r t)\right) \end{bmatrix} \tag{14}$$

$$LPF(i_{c\alpha} \times i_{c\beta}) = K_1 K_2 \sin(2\omega_r t) \tag{15}$$

where, $K_1 = A_c L_{dq}$ and $K_2 = A_c l_{dq}$

Furthermore (1) is delayed by $-\pi/4$, thus i_α and i_β are equal to:

$$i_{c\alpha}{}^{-\pi/4} = K_1 \sin(\omega_c t - \pi/4) + K_2 \sin(\omega_c t - 2\omega_a t + \pi/4) \tag{16}$$

$$i_{c\beta}{}^{-\pi/4} = -K_1 \cos(\omega_c t - \frac{\pi}{4}) - K_2 \cos(\omega_c t - 2\omega_a t + \frac{\pi}{4}) \tag{17}$$

Again by multiplying equations (16) and (17) and using a first order lowpass filter the conjugate of (15) is found:

$$LPF(i_{c\alpha} \times i_{c\beta})^{-\pi/4} = K_1 K_2 \sin(2\omega_r t + \frac{\pi}{2}) = K_1 K_2 \cos(2\omega_r t) \tag{18}$$

Once the signal is de-modulated, the resultant signals (15) and (18) can be normalised using the following trigonometric formula:

$$\sqrt{\left(K_1 K_2 \cos(2\theta_r)\right)^2 + \left(K_1 K_2 \sin(2\theta_r)\right)^2} = K_1 K_2 \tag{19}$$

Equations (15), (18) are divided by the resultant value of (19) and both signals are processed as follows:

$$i_h = \begin{pmatrix} \sin(2\omega_r t)\times\cos(\omega_h t) \\ +\cos(2\omega_r t)\times\sin(\omega_h t) \end{pmatrix} = \sin((\omega_h + 2\omega_r)t) \tag{20}$$

where ω_h is the shifting frequency and is equal to 3000 Hz

As a result the AM modulated signal (1) becomes FM

modulated (20), using the trigonometric identity equation, to improve the dynamics of the estimator. Finally, a simple PLL structure results, Fig. 5, composed of a phase detector followed by a first order filter and a Voltage Controlled Oscillator (VCO). The proposed PLL strategy is totally independent from any amplitude variation of the resultant current and can be used to detect the rotor speed and position of any salient-machine.

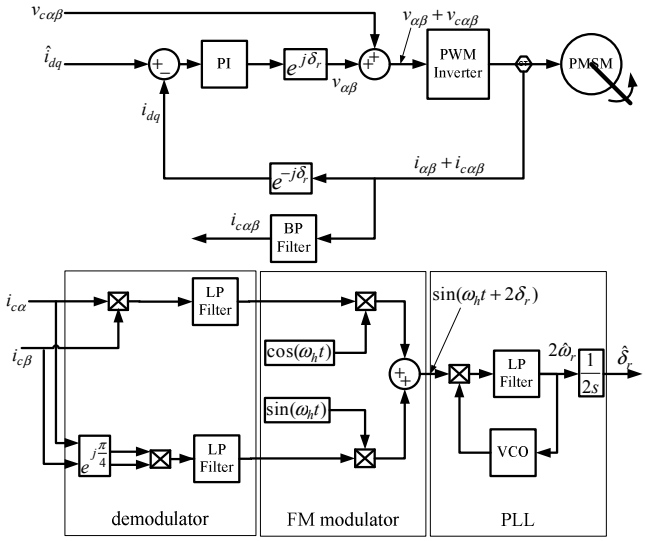

Fig.5: Block diagram of the proposed sensorless demodulation and PLL scheme

IV. Discussion and Results

The conventional PLL methods shown in Figs. 3-4 face some important drawbacks:

1. The variation of the d-q inductance values can change the amplitude of the modulated signal which affects the estimation process and sometimes requires retune of the conventional PLL [19, 20].
2. The Signal to Noise Ratio (SNR) of the resultant signal can vary depending on the saturation, the saliencies presented in the machine and the operating point of the machine, this can lead the PLL to loose track especially if the saliency/anisotropy becomes very small [21].
3. Tuning the PI parameters of the PLL require sometimes the knowledge of the inductance values, to normalise the PLL input signal and improve the dynamics of the PLL [18].
4. The inverter nonlinearity affects the estimation process and lead to erroneous position estimation [22, 23].

As studied previously and is shown in (15) it is possible to demodulate (1) without using the conventional heterodyning demodulation method and hence avoid some of the previously mentioned problems. Therefore, a sensorless PMSM drive has been modelled using Matlab/Simulink to validate the proposed estimation method and compare it with the conventional algorithms.

Table. I
Motor Parameters

Symbol	Quantity	Value (unit)
P	Pole pair	2
R_s	Stator resistance	6.25 (Ω)
l_d	Stator d-axis inductance	142 (mH)
l_q	Stator q-axis inductance	380 (mH)
ω_{rated}	Rated speed	6000 (rpm)

The injected carrier signal oscillates at 1000 Hz and the amplitude is 50 V. The bandpass digital IIR filters are designed to have a 200 Hz bandwidth and be centred at 1000 Hz. The PI controller has been tuned for both open loop and closed loop PLL structures by trial and error to get the appropriate results for accurate speed and position. However, the proposed demodulation and estimation method requires only setting the high frequency shift ω_h value and tune the VCO of the PLL once for any operating point. The drive is subjected to a ramp command speed at the start and then a constant value of 2.5 Hz. Such a test can help to evaluate the estimators at different speed conditions. The actual speed response of the system and the estimated speed of the open loop, closed loop, and proposed PLL are shown in Figs. 6-8 respectively. These tests have been done at constant amplitude of the injected signal and the results show that the proposed method does not exhibit the rippling in the speed estimation as seen with the conventional methods. This is because the disturbance and noise affecting the estimation process can be eliminated from the input signal to the PLL (15).

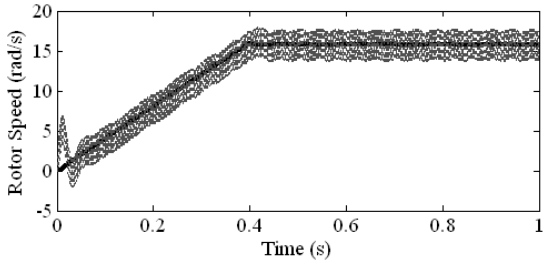

Fig.6: Actual (bold line) and estimated speed (dash) of the open loop PLL

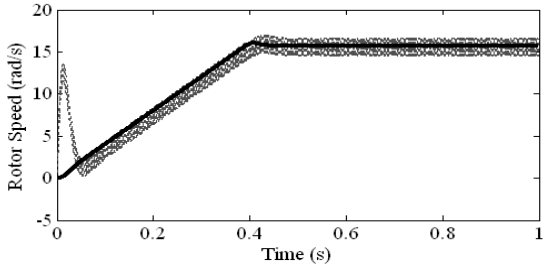

Fig.7: Actual (bold line) and estimated speed (dash) of the closed loop PLL

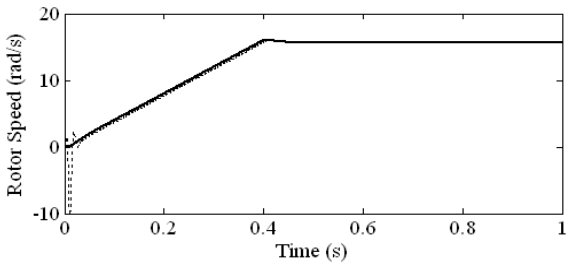

Fig.8: Actual (bold line) and estimated speed (dash) of the proposed demodulation and PLL strategy

Once the speed is detected accurately, the position can be determined by using an integrator. The results of the actual and estimated rotor position of the three methods are shown in Figs.9-11.

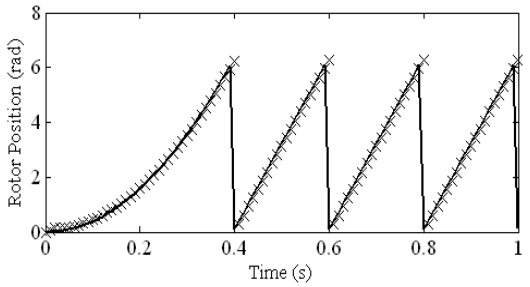

Fig.9: Actual (bold line) and estimated position (x) of the open loop PLL

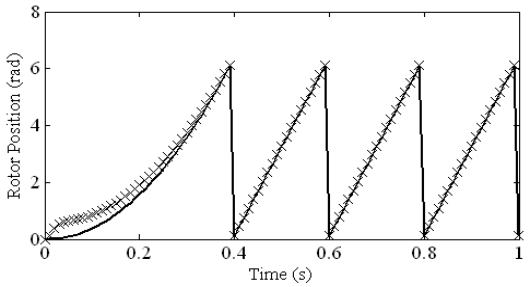

Fig.10: Actual (bold line) and estimated position (x) of the closed loop PLL

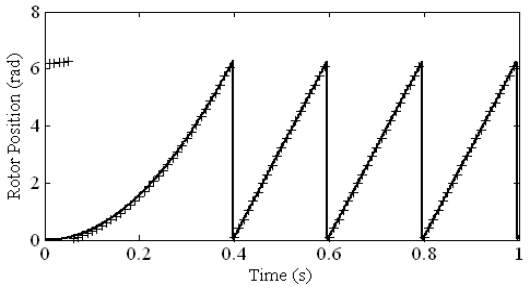

Fig.11: Actual (bold line) and estimated position (x) of the proposed scheme

The previous tests have shown that the three estimators are able to lock on the rotor position but with superior accuracy, using the proposed method. However, it is important to compare between the conventional and new methods in case there is an amplitude change of the current ($A_c\, I_{dq}$) as is mentioned at the beginning of this section. One suggestion is to decrease the voltage amplitude of the injected signal (decrease the SNR) gradually (20% each 0.1s), as it is proportional to the current amplitude, and observe the effect on the estimation process. It can be clearly seen in Figs. 12-15 that the estimated position is delayed until a certain low current amplitude, then the PLL loose track completely. On the other hand the proposed method maintains accuracy of the estimated speed and position and stability of the PLL when the current amplitude varies, as it appears in Figs.16-17. However the transient that appears in the speed and position response Fig.16 is due to a sudden change of the voltage amplitude. Such a transient cannot be eliminated by simple filters. More sophisticated signal processing schemes such as Wavelet de-noising [24] can be used to reduce the effect of such disturbances and improve the accuracy of the proposed estimation method.

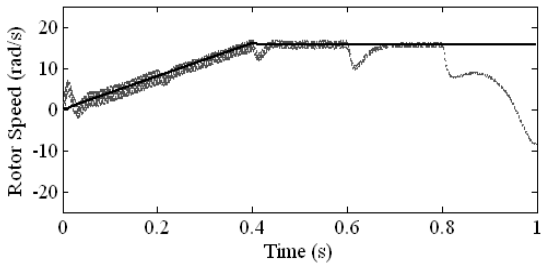

Fig.12: Actual (bold line) and estimated speed (dash) of the open loop PLL when the current amplitude is decreased gradually

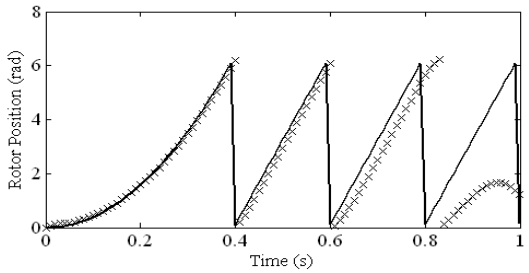

Fig.13: Actual (bold line) and estimated position (x) of the open loop PLL when the current amplitude is decreased gradually

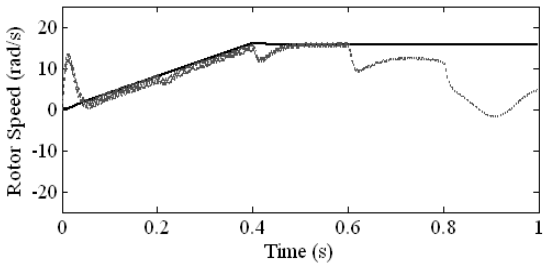

Fig.14: Actual (bold line) and estimated speed (dash) of the closed loop PLL when the current amplitude is decreased gradually

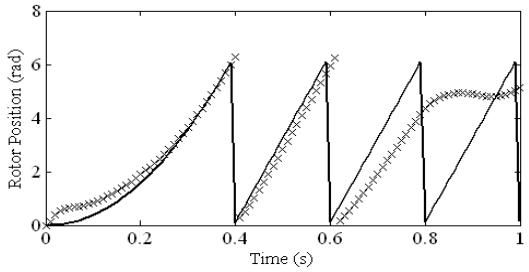

Fig.15: Actual (bold line) and estimated position (x) of the closed loop PLL when the current amplitude is decreased gradually

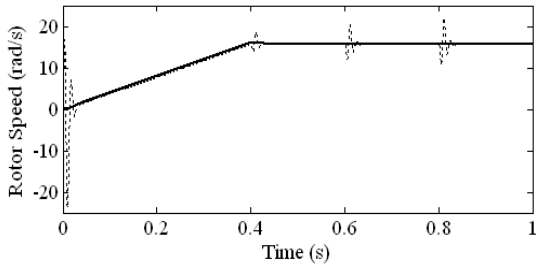

Fig.16: Actual (bold line) and estimated speed (dash) of the proposed demodulation and estimation method when the current amplitude is decreased gradually

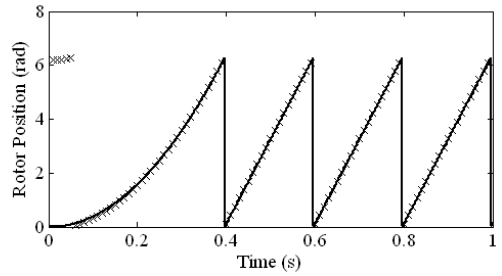

Fig.17: Actual (bold line) and estimated position (x) of the proposed demodulation and estimation method when the current amplitude is decreased gradually.

V. CONCLUSION

In general, high frequency injection methods are known to be parameter independent. However, it has been shown that an amplitude variation in the high frequency current response during the estimation process can lead to erroneous results, while using the conventional PLL methods. This is due to the relation between the current amplitude and the response of the estimator. The proposed demodulation is used to normalise the carrier signal, without the knowledge of the machine parameters, and the PLL used to detect the rotor speed and position more accurately than the conventional methods. Finally it is important to note that the proposed method can be used for any salient synchronous machine under any operating conditions and can be extended to a higher speed range.

REFERENCES

[1] J. W. Finch and D. Giaouris, "Controlled AC Electrical Drives," *IEEE Transactions on Industrial Electronics*, vol. 55, pp. 481-491, 2008.

[2] M. Barut, S. Bogosyan, and M. Gokasan, "Speed-Sensorless Estimation for Induction Motors Using Extended Kalman Filters," *IEEE Transactions on Industrial Electronics*, vol. 54, pp. 272-280, 2007.

[3] M. Cirrincione and M. Pucci, "An MRAS-based sensorless high-performance induction motor drive with a predictive adaptive model," *IEEE Transactions on Industrial Electronics*, vol. 52, pp. 532-551, 2005.

[4] B. Nahid-Mobarakeh, F. Meibody-Tabar, and P. M. Sargos, "State and disturbance observers in mechanical sensorless control of PMSM," presented at IEEE ICIT '04. International Conference on Industrial Technology, 2004.

[5] S. Maiti, C. Chakraborty, Y. Hori, and M. C. Ta, "Model Reference Adaptive Controller-Based Rotor Resistance and Speed Estimation Techniques for Vector Controlled Induction Motor Drive Utilizing Reactive Power," *IEEE Transactions on Industrial Electronics*, vol. 55, pp. 594-601, 2008.

[6] J. Cilia, G. M. Asher, K. J. Bradley, and M. Sumner, "Sensorless position detection for vector-controlled induction motor drives using an asymmetric outer-section cage," *IEEE Transactions on Industry Applications*, vol. 33, pp. 1162-1169, 1997.

[7] A. Zentai and T. Daboczi, "Improving INFORM calculation method on permanent magnet synchronous machines," presented at IEEE Instrumentation and Measurement Technology Conference Proceedings, 2007.

[8] T. M. Wolbank, M. A. Vogelsberger, and R. H. Stumberger, "Adaptive Flux model for commissioning of signal injection based zero speed sensorless flux control of induction machines," presented at 7th International Conference on Power Electronics and Drive Systems PEDS '07., 2007.

[9] K. D. Hurst and T. G. Habetler, "Sensorless speed measurement using current harmonic spectral estimation in induction machine drives," *IEEE Transactions on Power Electronics*, vol. 11, pp. 66-73, 1996.

[10] C. Nitayotan and S. Sangwongwanich, "A filtered back EMF based speed-sensorless induction motor drive," presented at Thirty-Sixth IAS IEEE Annual Meeting Industry Applications Conference, 2001.

[11] P. L. Jansen and R. D. Lorenz, "Transducerless field orientation concepts employing saturation-induced saliencies in induction machines," *IEEE Transactions on Industry Applications*, vol. 32, pp. 1380-1393, 1996.

[12] W. Limei and G. Qinging, "Principles and implementation of permanent magnet synchronous motor zero-speed sensorless control," presented at 7th International Workshop on Advanced Motion Control, 2002.

[13] C. Silva, G. M. Asher, and M. Sumner, "Hybrid rotor position observer for wide speed-range sensorless PM motor drives including zero speed," *IEEE Transactions on Industrial Electronics*, vol. 53, pp. 373-378, 2006.

[14] G. El-Murr, D. Giaouris, and J. W. Finch, "Totally Parameter Independent Speed Estimation of Synchronous Machines Based on Online Short Time Fourier Transform Ridges," *IAENG Engineering Letters*, vol. 16, pp. 90-95, 2008.

[15] T. Aihara, A. Toba, T. Yanase, A. Mashimo, and K. Endo, "Sensorless torque control of salient-pole synchronous motor at zero-speed operation," *IEEE Transactions on Power Electronics*, vol. 14, pp. 202-208, 1999.

[16] A. Consoli, G. Scarcella, and A. Testa, "Industry application of zero-speed sensorless control techniques for PM synchronous motors," *IEEE Transactions on Industry Applications*, vol. 37, pp. 513-521, 2001.

[17] O. C. Ferreira and R. Kennel, "Encoderless Control of Industrial Servo Drives," presented at 12th International EPE-PEMC. Power Electronics and Motion Control Conference, 2006.

[18] H. W. de Kock, M. J. Kamper, O. C. Ferreira, and R. M. Kennel, "Position sensorless control of the Reluctance Synchronous Machine considering High Frequency inductances," presented at 7th International Conference on Power Electronics and Drive Systems, PEDS '07, 2007.

[19] J. Hu, L. Xu, and J. Liu, "Eddy Current Effects on Rotor Position Estimation for Sensorless Control of PM Synchronous Machine," presented at 41st IAS Annual Meeting of the IEEE Industry Applications Conference, 2006.

[20] P. Guglielmi, M. Pastorelli, and A. Vagati, "Cross-Saturation Effects in IPM Motors and Related Impact on Sensorless Control," *IEEE Transactions on Industry Applications*, vol. 42, pp. 1516-1522, 2006.

[21] F. Briz, M. W. Degner, A. Diez, and R. D. Lorenz, "Static and dynamic behavior of saturation-induced saliencies and their effect on carrier-signal-based sensorless AC drives," *IEEE Transactions on Industry Applications*, vol. 38, pp. 670-678, 2002.

[22] J. Holtz, "Initial Rotor Polarity Detection and Sensorless Control of PM Synchronous Machines," presented at 41st IAS Annual Meeting of the 2006 IEEE Industry Applications Conference, 2006.

[23] J. M. Guerrero, M. Leetmaa, F. Briz, A. Zamarron, and R. D. Lorenz, "Inverter nonlinearity effects in high-frequency signal-injection-based sensorless control methods," *IEEE Transactions on Industry Applications*, vol. 41, pp. 618-626, 2005.

[24] D. Giaouris, J. W. Finch, O. C. Ferreira, R. M. Kennel, and G. M. El-Murr, "Wavelet Denoising for Electric Drives," *IEEE Transactions on Industrial Electronics*, vol. 55, pp. 543-550, 2008.